Progress in the design of the superconducting magnets for the EU DEMO

EU Progress in Superconductor Technology Development for DEMO Magnets

V. Corato [a],T. Bagni[b], M. E. Biancolini[c], R. Bonifetto[d], P. Bruzzone[e], D. Ciazynski[f], M. Coleman[g], A. della Corte[a], A. Di Zenobio[a], A. Dembkowska[h], M. Eisterer[i], W.H. Fietz[l], D. X. Fischer[i], E. Gaio[m], L. Giannini[a], F. Giorgetti[c], R. Heller[l], B. Lacroix[f], M. Lewandowska[h], A. Maistrello[m], L. Morici[a], L. Muzzi[a], A. Nijhuis[b], F. Nunio[f], A. Panin[n], L. Savoldi[d], K. Sedlak[e], B. Stepanov[e], G. Tomassetti[a], A. Torre[f], S. Turtù[a], D. Uglietti[e], R. Vallcorba[f], K.-P. Weiss[l], R. Wesche[e], M.J. Wolf[l], K. Yagotintsev[b], L. Zani[f], and R. Zanino[d].

[a]ENEA, 00044 Frascati, Italy
[b]Univ. of Twente, 7522 Enschede, Netherlands
[c]University of Rome Tor Vergata, 00133 Rome, Italy
[d]NEMO group, Dipartimento Energia, Politecnico di Torino, 10129 Torino, Italy
[e]EPFL/SPC, 5232 Villigen, Switzerland
[f]Commissariat à l'Energie Atomique et aux Energies Alternatives, France
[g] EUROfusion, 85748 Garching bei München, Germany
[h]West Pomeranian University of Technology, Szczecin, 70310 Szczecin, Poland
[i]TUW, Wien, Austria
[l]KIT, 76344 Eggenstein-Leopoldshafen, Germany
[m]Consorzio RFX, 35127 Padova, Italy
[n]IEK-4 - Plasma Physics, Forschungszentrum Juelich GmbH, D52425 Juelich, Germany

In the framework of the DEMOnstration Fusion Power Plant (DEMO) program launched by the EUROfusion consortium, a pre-conceptual design of the superconducting magnet system has been developed. For the toroidal field coils (TFCs), three winding pack (WP) options have been proposed; exploring different winding approaches (pancakes vs. layers) and manufacturing techniques (react & wind vs. wind & react Nb_3Sn). Thermal-hydraulic and mechanical analyses on the three WPs have given encouraging results, with some critical issues to be solved in the future studies and optimization. The experimental tests on TF prototype short sample conductors have demonstrated a limited performance degradation with electro-magnetic cycles and an effective strain much lower than the one assessed in most of the large-size Nb_3Sn conductors reported in literature. The Toroidal Field quench protection circuit has been studied, starting from different topologies and focusing on the most promising one. Two designs are also presented for the central solenoid magnet, with preliminary evaluations on the AC losses during the plasma breakdown.

Finally, the design of a TF winding pack based on HTS conductors and the experimental tests on "fusion-relevant" HTS cables are illustrated.

Keywords: nuclear fusion, DEMO, superconducting magnets.

1. Introduction

In the framework of the Roadmap to Fusion Electricity Horizon 2020 [1], EUROfusion consortium is supporting a comprehensive design study of a DEMOnstration Fusion Power Plant (DEMO) [2] with the aim to demonstrate that a fusion reactor can produce net electrical power and supply energy to the grid.

This paper reports on the state of the art in the pre-conceptual design of the DEMO magnet system, focusing on the progresses obtained after the results already mentioned in [3]. In Section 2 three configurations for the Toroidal Field (TF) winding packs (WP) are proposed, based on different winding schemes (layer vs pancake) and Nb_3Sn manufacturing technology (wind & react (W&R) vs react & wind (R&W)). For each configuration thermal-hydraulic and mechanical analyses are included, as well as the results of the R&D activity on short-size samples, when available. Preliminary studies on different possible topologies of the TF Quench Protection Circuit (QPC) are presented in Section 3. Section 4 reports on two proposals for the design and preliminary analyses of the Central Solenoid (CS) coils. The design and the experimental activity on High Temperature Superconductor (HTS) conductors relevant to fusion program are illustrated in Section 5. Finally, conclusions are drawn.

author's email: valentina.corato@enea.it

2. TF coils pre-conceptual design and R&D

In this section three designs for the Toroidal Field (TF) coils are proposed, namely WP#1, WP#2 and WP#3. All designs refer to the 2015 reference baseline for DEMO reactor [4]. Anyway some of the short length samples, already manufactured and tested, are based on the previous design (2013 reference baseline [5]), characterized by different requirements. Scope of these R&D program and experimental campaigns was anyhow to demonstrate the feasibility and performances of new technologies, rather than qualify a conductor layout for a specific requirement.

2.1 TF WP#1 design

The WP#1 [6], [7] is based on the React&Wind (RW) method for Nb_3Sn magnets, that is the conductor is wound after the heat treatment, which is carried out without stainless steel (SS) conduit and electrical insulation. The WP is wound in single layers (SL); this approach allows the grading of both superconductor (SC) and SS cross section in the different layers, depending on the magnetic field and the local stress value, respectively. In particular, with decreasing distance from the plasma the SC content decreases, thus optimizing the use of SC as function of the local magnetic field, whereas the jacket thickness increases to withstand the higher mechanical stresses [8], [9].

As shown in figure 1(a), the WP layout consists of 12 layers×19 turns (17 turns in the last layer), i.e. in total 226 turns, allowing a conductor operating current of 63.3 kA.

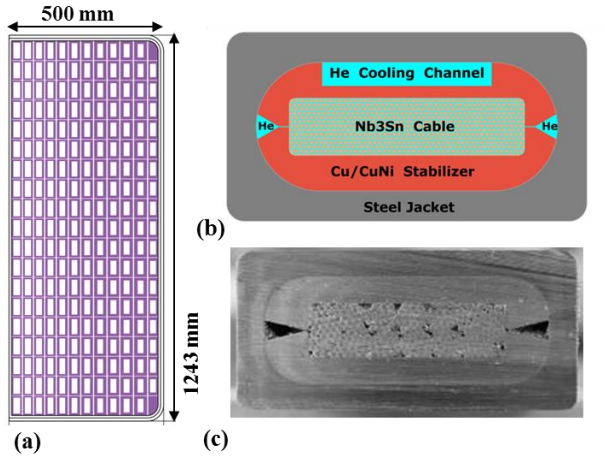

Fig.1 (a) TF WP#1 configuration (b) Cross section of the RW1 conductor (c) Cross section of the RW2 conductor.

The conductor, namely RW2, has a flat shape, to keep the SC strands close to the neutral bending axis, and two SS shells, assembled by longitudinal laser welding. Two solid profiles of Cu/CuNi mixed matrix are used as stabilizer. The layout of the RW2 conductor is listed in Table I, in comparison with the main parameters of the first prototype, namely RW1, designed for the previous DEMO reference baseline [5].

Table 1. Main parameters the RW1 and RW2 conductors for the highest field layer

Layout	RW1	RW2
Operating Current [kA]	82.4	63.3
Peak Operating Field [T]	13.3	12.23
Width x Height [mm x mm]	100x34	61.5x32.1
Strand Diameter [mm]	1.5	1.2
Number SC strands	306	234
Number Cu strands	17	13
SC cable size [mm x mm]	62,0 x 12,3	35 x 11
Void fraction in cable [%]	27	23
Jcopper [A/mm^2]	119	90
Jnon-copper [A/mm^2]	305	478
Central strip in flat cable	none	steel
Steel cross section [mm^2]	2060	893.5
Conduit inner radius [mm]	3	8

The thermo-hydraulic analyses [10],[11] have been carried out on the proposed WP design considering a nuclear heating load $P_{NH}(r) = 50\exp(-r/140)$ W/m^3, as a function of the radial distance r (in mm) from the plasma facing wall [12]. The conductor is modelled as a 1-D system of several parallel components – three thermal components (strands, Cu/CuNi stabilizer and steel jacket) and three hydraulic components (He in the bundle, He in the triangular side cooling channels, and He in the upper rectangular channel). Heat transfer between the solid components is set to 500 W/(m^{2}K), where the contact surface between strands and copper stabilizer is assumed to be 1/5 of the overall boundary area. The heat transfer coefficient between helium and solid components in turbulent flow is derived from the Dittus-Boelter correlation [13]. Also the friction correlations and heat transfer coefficients in laminar regime, which may become relevant in part of the conductor during quench transient, are specified in [13]. In normal conditions, the temperature margin ΔT_{marg}^{min} of all conductors exceeds the required 1.5 K minimum value [14]. In off-normal conditions, the quench hot spot temperature, T_{hs}, is safely below the acceptable limit of 150 K specified for the steel conduit.

Concerning mechanical analysis, critical locations are mapped on outer leg and inboard leg, indicated as points 1 and 2, respectively, in Fig. 2(a). Jacket critical paths are shown in Fig. 2b, with corresponding results. On the outboard, mostly due to the coil out-of-plane bending , the primary membrane stress for WP#1 (692 MPa) slightly exceeds the allowable static stress for chosen structural steel (667 MPa), whereas on the inboard leg, where radial and toroidal compressions act in addition to poloidal tension, there are no issues with the jacket static strength. As a matter of fact, this design was already the result of a first pre-optimization study [8], [9]. As a first step to study the critical locations in insulation, the shear stress coupled with compression has been considered so far. In respect to the shear stress criteria, the insulation static strength is not that critical, but the cyclic shear stress could be an issue for WP#1 coil, since the layout has not enough bending stiffness in respect to the in-plane and the out-of-plane loading.

As a possible countermeasure, the coil in-plane bending may be decreased by its re-shaping, whereas the coil lateral bending is decreased by either stiffening the outer inter-coil

structures (OIS) or by increasing the coil case bending stiffness.

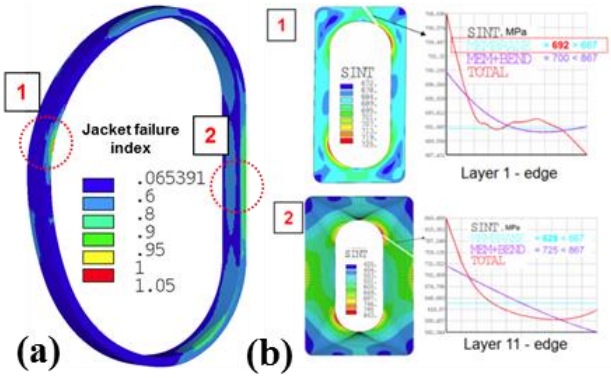

Fig. 2 (a) Mechanical critical locations in TF WP#1 (b) Jacket critical paths, with corresponding results.

Two short-length samples, namely RW1 and RW2 as reported above, were manufactured and tested. The DC test includes I_c and T_{cs} runs before and after 1100 load cycles and a warm-up/cool-down (WUCD).

Results after WUCD of 2016 experimental campaign for RW1 sample are reported in figure 3[6]. The "effective strain", ε_{eff}, is the parameter to be used in the strand scaling law to fit the conductor performance. For RW1, the black and red dashed lines in figure 3 give the performance assessment at ε = -0.28% and ε = -0.35% for the left and right legs, respectively. The T_{cs} at the nominal operation point (I_{op}=82.4A, B_{eff}=13.3T) is between 7.1-7.3K, well above the required 6.5 K minimum value.

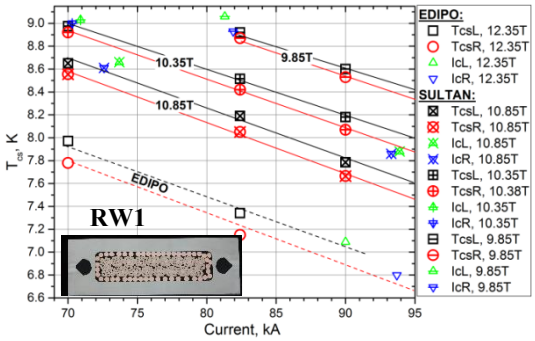

Fig. 3 I_c and T_{cs} results after the WUCD for RW1 sample.

Concerning RW2 sample [7], the nominal operating point (I_{op}=63.3 kA, B_{eff}=12.23 T) cannot be achieved in the SULTAN test facility. The cyclic loading is thus applied at the equivalent transverse load condition of 70 kA and 10.9 T. The T_{cs} at the nominal operating point is extrapolated, providing a value of about 6.4 K. The evolution of the T_{cs} with cycles, shown in figure 4(a), presents a degradation of ≈0.25K, presumably due to a shift in the strain distribution. In fact, the index of the superconducting transition remain stable at n = 18, excluding the filament breakage as an explanation for the performance loss. For the RW2 the assessment of the effective strain is ≈ -0.40 %. The AC losses measured on the RW2 sample (figure 4b) are very low, giving a coupling loss constant $n\tau$ ≈50 ms. This suggests a possible use of the same layout also for a CS conductor.

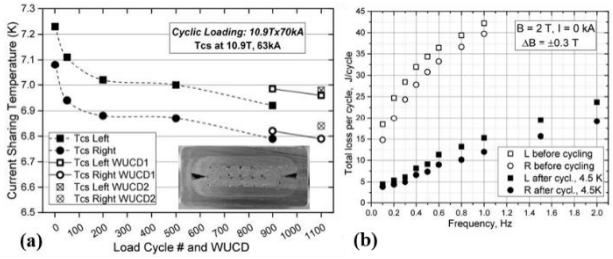

Fig. 4 (a) Evolution of T_{cs} with load cycles and (b) total AC losses per cycle vs. frequency, measured on RW2 sample.

2.2 TF WP#2 design

The WP#2, sketched in figure 5(a), has also a layer-wound, graded structure, but based on 6 Nb_3Sn double-layers (DL), and a WR CICC concept. The total number of turns is in this case 202, with a conductor operating current, I_{op}=70.8 kA at 4.5K and 12.3T. The approach to the design of the cables is represented in figure 5(b) [15]: the segregated copper is either distributed within the cable bundle, with 1.0 mm diameter wires, or within the cores of the petals (C1), with 1.5 mm diameter wires, or within the overall cable core (C2), again with 1.5 mm diameter wires. The cable is formed with six petals around core C2, but 2 out of the 6 petals have a spiral (low-impedance cooling channels) as a core. Main geometrical parameters of TF WP#2 are summarized in Table 2 and the target void fraction in the cable bundle region is 0.26% for all conductors.

Comprehensive thermo-hydraulic analyses have been carried out on the proposed WP design considering the nuclear heating load reported in [12]. The model, described in greater detail in [16],[17], includes the 1D flow of supercritical He in each of the thermally coupled layers of the WP and in the casing cooling channels (CCC), the heat conduction in the casing and the external cryogenic circuits for both WP and casing with quench lines. Moreover, the model accounts for both eddy currents heat deposition in the casing and AC losses in the cable induced by the fast discharge triggered by the quench protection system. The nominal pulsed scenario [18] is implemented for simulations. As shown in figure 5(c), in normal operating conditions at the end of flat-top (EoF) the ΔT_{marg}^{min} requirement of 1.5 K is satisfied in all the conductors, but, the NH during cyclic operation erodes the initial steady state value of about 0.1÷0.4 K, depending on the distance from the plasma.

In off-normal operation, the design satisfies the 150 K maximum T_{hs} criterion, considering also a collapse of the relief channels in the WP and a plugging of selected CCCs at critical locations. Even with a reduction of the available cooling, the corresponding erosion of the ΔT_{marg}^{min} remains in all cases marginal (<0.1 K).

Mechanical loads on WP#2 have been analyzed using the Stress Recovery Tool (SRT) [19]. This method is supposed to obtain reliable structural results from simplified models, with consistent time saving with respect to full-detailed analyses. A hierarchical approach is envisioned: complete analysis of the TF coil D shape

is conducted using a simplified model that adopts smeared properties for the mechanical analysis of the WP; results are then transferred to a full detailed model of a slice of WP so that an accurate stress recovery can be enabled.

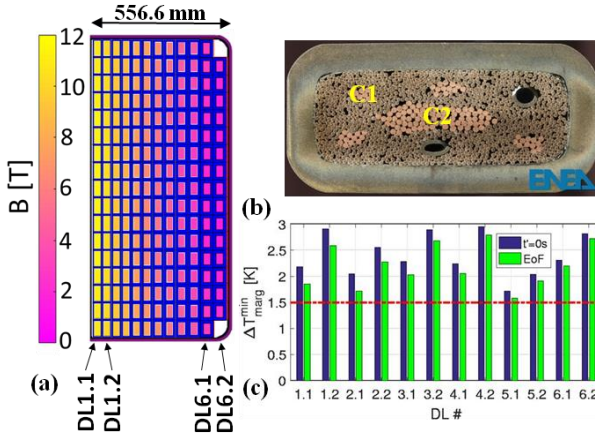

Fig.5 (a) TF WP#2 configuration (b) Cross section of the SC conductor (c) ΔT_{marg}^{min} in all layers before the plasma burn start at t'=0 s (blue bars), and at EoF of a periodic pulse (green bars).

Table 2. TF WP#2 reference conductor design. Where different, the values for the first and second layer of the same DL are separated by "/".

Data	DL1	DL2	DL3	DL4	DL5	DL6
N. SC strands (D=1 mm)	720	360	270	180	120	120
Strand Cu:nonCu	1	1	1	1	1	1
N. Cu strand (D=1 mm)	360	720	540	630	690	690
N. Cu strand (D=1.5 mm)	108	48	138	120	84	84
Jacket thickness [mm]	3.9	5.3	6.8	8.4	10.0	11.7
Turn length [m]	44/ 44.3	44.5/ 44.8	45 / 45.3	45.5/ 45.8	46.1/ 46.4	46.7/ 47.1
# turns	17/17	17/17	17/17	17/17	17/17	17/15
Hydraulic length [m]	748/ 753	757/ 761	765/ 770	774/ 779	784/ 789	794/ 706

On the casing the stress hot spots are located under the OIS junctions (800 MPa in terms of Tresca stress) and on the sharp edges of inner leg straight portion (Tresca stress of about 750 MPa), both higher than the allowable value (667 MPa). The local analysis shows that the average stress computed by the SRT is always below the allowable value (with a safety factor, SF, ~1.6), whereas the peak stress exceeds the limits in the inner corner of the jacket. The shear stress for insulation also exceeds the limits (54MPa) in a few critical points, with a peak of 98 MPa.

To demonstrate the technological feasibility of large-size, high current conductors relevant to DEMO magnets, a short-length sample was manufactured and tested in the EDIPO facility [15]. The Cable-in-Conduit Conductor (CICC) was designed for accomplishing the 2013 reference baseline [5], i.e. to operate at 81.7 kA in an effective field of about 13 T (with peak field of 13.5 T), and up to a temperature of at least 6.5 K. The T_{CS} evolution with the e.m. load cycles is shown in figure 6. It's worth noting that the T_{CS} is not affected by degradation with cycles.

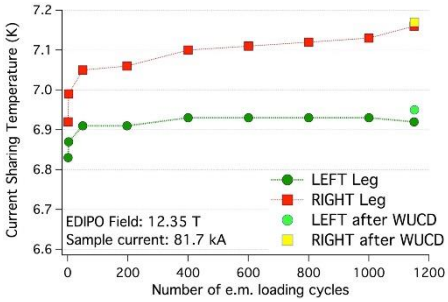

Fig.6 T_{CS} vs. number of electromagnetic loading cycles for the two legs of TF WP#2 sample. At the last cycle, an additional measurement is done after the warm-up/cool-down procedure (WUCD).

The behavior of T_{CS} vs. the operating current at different background magnetic field values was compared with the T_{CS} curves computed starting from $I_c(\varepsilon,T,B)$ data collected at the University of Twente on the employed strands [20]. The comparison provides an effective total strain value in the range: - 0.55% ÷ - 0.50%, that corresponds to the design target.

AC losses were measured by using both calorimetric and magnetization methods [15],[21], with the magnetic field orientation either perpendicular or orthogonal to the wide conductor side. The energy deposited per cycle and per unit volume is rather high, with a pronounced difference depending on the orientation. Moreover, only a minor reduction in the losses is observed with cycling, differently from the behavior normally exhibited by ITER conductors [22]. This unclear aspects deserve a wider investigation on further samples.

2.3 TF WP#3 design

The TF WP#3 consists of 9 double pancakes (DP) wound in 9 turns per pancake based on Nb_3Sn W&R fabrication process [23]. The TF conductor proposal is an ITER-type 88kA CICC, with a central spiral inserted in a thick square stainless steel jacket to compensate the absence of radial plates. Figure 7 shows the TF WP and the conductor, whose main characteristics are summarized in table 3.

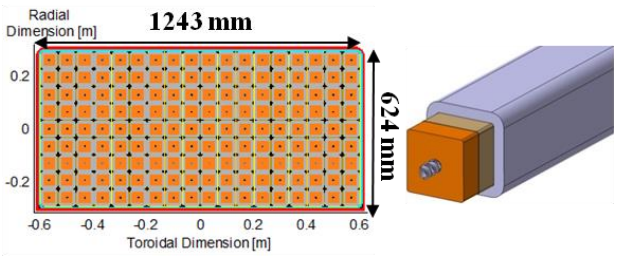

Fig.7 TF WP#3 reference structure and conductor design

Thermal-hydraulic studies have been carried out both in normal and off-normal operating conditions [24],[25].

The simulations of a 2 hour burn, focused on both central and lateral clock-wise (CW) pancakes, allowed to

assess the ΔT_{marg}^{min} . In presence of CCC the 1.5 K criterion is respected, whereas it slightly fails in the central CW if CCC are not included. Figure 8 summarizes the time evolution of the temperature margin.

Table 3. TF WP#3 reference conductor design.

Parameter	Value
Operating Current [kA]	88
Peak Operating Field [T]	12.27
Strand Diameter [mm]	0.984
Cr plating [μm]	2
Number SC strands	828
Number Cu strands	790
Cos (θ)	0.95
Cable Size [mm]	43.62
Void Fraction in cable [%]	30
Jacket thickness [mm]	9.43
Hydraulic length [m]	408

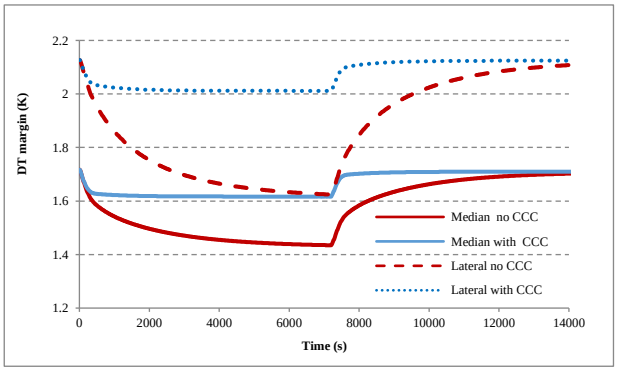

Fig.8 Time evolution of the temperature margin with or without CCC.

If the radial thermal coupling from turn to turn and between adjacent pancakes, is implemented in the model, the ΔT_{marg}^{min} decreases of about 0.07 K, showing the effect of radial thermal exchanges inside the winding pack is limited.

Several quench scenarios were simulated, considering a heat deposition either on the internal turn (high field and low ΔT_{marg}^{min}) for both median and lateral pancakes or at the middle of hydraulic length (lower field and higher ΔT_{marg}^{min}) for the median pancake. In all cases, the disturbance was 1 meter long and lasted 100 ms, and the quench was initiated with twice the minimum quench energy. The T_{hs} criterion was satisfied for all cases, except when the quench was initiated at middle of conductor, at rather low field.

A mechanical analysis similar to the one presented for WP#1 has been done for WP#3[9]. As shown in figure 9, on the outboard leg membrane stress for WP#3 is safely below the allowable stress (point 1 of figure 9 (b)), whereas on the inboard leg (point 2) the sum of the membrane stress plus bending (914 MPa) exceeds the static limit of 867 MPa. In addition a detailed mechanical analysis of the cumulative radial stress in the conductor jacket [23] has been performed. The static stress criteria is fulfilled by increasing the jacket inner radius from 2 mm to 6 mm, thus decreasing the bending of the conductor walls.

The short length sample of the WP#3 conductor is under manufacture and will be tested in 2018.

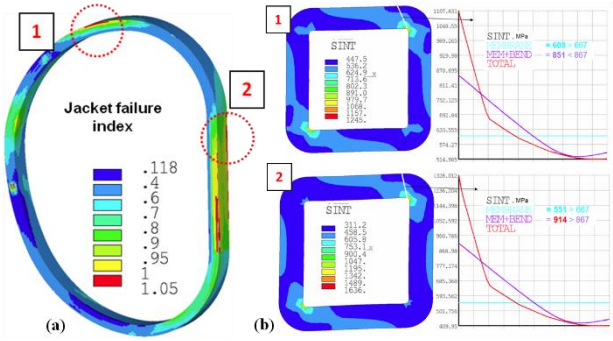

Fig. 9 (a) Mechanical critical locations in TF WP#3 (b) Jacket critical paths, with corresponding results.

3. Preliminary TF Quench Protection circuit

Four alternative topologies (called A, B, C and D in figure 10) have been proposed for the DEMO TF quench protection circuit (QPC) [26], as shown in figure 9. The main differences are in the grounding system (ITER-like or JT-60SA like) and in the connection of the discharge resistors, that can be in parallel to the QPC circuit breaker or to the coil. In all cases, when the QPC intervenes, the terminal-to-ground voltage is half the voltage across the coil.

The simulations provide the voltage waveforms at the coil terminals, across the coils and the Joule integral parameter, i^2t, in the coils during the discharge, both for the 18 and 9 sectors cases.

Considering 18 sectors, in the more critical operating condition (QPC intervention failure and ground fault opposite to faulted QPC) the terminal-to-ground voltage for topologies A (12.1 kV), B (11.6 kV) and C (11.8 kV) is 2.5 time higher than that one in case of regular QPC intervention (4.4 KV). On the contrary, with topology D, the terminal-to-ground voltage is of 8.8 kV, that is only two times the value reached in case of regular QPC intervention. If 9 sectors are considered, the trend is the same, but all values are doubled.

With topologies C and D the overall resistance remains the same in all the operating conditions, thus the discharge constant time is not modified and therefore there is not an increase in the i^2t.

In all cases, the peak voltage values at the coil terminals is 8.8kV for 18 sectors. This voltage increases to 17.6 kV in the case with 9 sectors, which exceeds the limits presently assumed (10 kV) for the TF coil insulation design, thus suggesting to maintain the present reference TF circuit topology with 18 sectors.

However, it worth noting that all these analyses have been carried out assuming resistors with constant resistance. If resistors having a variable resistance with temperature were adopted, like done both for ITER and JT-60SA, the peak voltage value could be significantly reduced. In the future this solution will be explored for DEMO, in order to reduce the number of sectors, with the accompanying advantages in terms of cost and size

of the protection system, penetrations in the tokamak building, bus-bars and current leads.

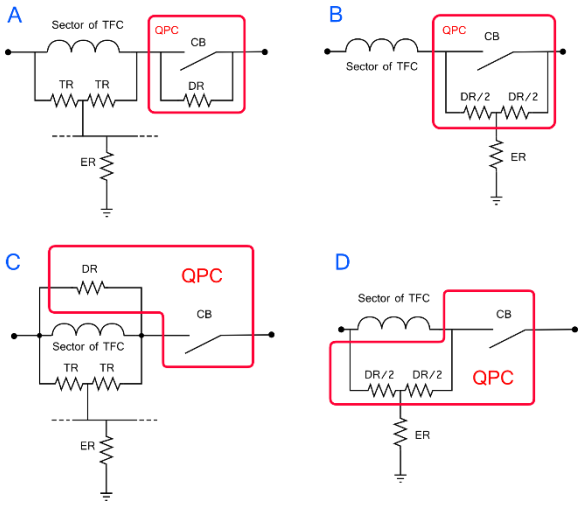

Fig. 9 Circuit topologies: A is ITER-like, B is JT-60SA like, C and D differ from A and B respectively for having the discharge resistor connected in parallel to the relevant TFC sector.

4. CS coils pre-conceptual design

As for the TF, the CS should fulfill the geometrical and operative requirements defined by the system code PROCESS [4]. The required geometry is a 5 modules CS (with a central double module), that should provide a total magnetic flux $\Phi_{CS} = 320$ Wb. Two designs are presented for the Central Solenoid (CS) magnet, as reported below.

4.1 Nb_3Sn based CS design

A first design based on a pancake wound Nb_3Sn conductor has been proposed for the CS coils [23]. The external radius has been fixed to 3.2 m in order to take into account the gap between TF and CS, used to accommodate mechanical deformation of TF as well as pre-compression tie-plates. The design is based on the CSJA6 Nb_3Sn strand, in order to exploit the experimental results obtained for ITER R&D [27]. The main parameters of the CS WP and conductor are presented in Table 4.

The burn scenario has been simulated [24] considering 80 s premagnetisation, 2 hours burn and 10 minutes dwell. Coupling and hysteresis AC losses have been computed to assess the temperature margin. The minimum value, found at the end of 1st turn and at the end of the dwell, was 1.42 K for $n\tau$=638 ms, that is the time constant value deduced from ITER CS insert tests performed at CSMC Naka in 2015 [27]. The sensitivity analysis has shown that $n\tau$ should decrease to 250 ms to fulfill the 1.5 K criterion.

Also the AC losses during the breakdown CS current variation have been computed [28] considering a variation at the maximum external magnetic field of 1.7 T/s during 0.8 seconds [29]. The ΔT_{marg}^{min} drops heavily below 1.5K unless the $n\tau$ is reduced to 200 ms. Considering the screening current effect in cable, that attenuates the external field variation inside the cable, the power deposited is highly reduced and the ΔT_{marg}^{min} is around the limit. Anyway the breakdown phase is a critical step from the point of view of the CS temperature margin and deserves further analysis.

Table 4. Nb_3Sn CS conductor and WP design.

Parameter	Value
Conductor size [mm]	61
Conductor current [kA]	55.5
Jacket thickness [mm]	12.8
Number SC strands	659
Number Cu strands	596
Number of turns	13
Number of pancakes in the CS	266
External radius of the CS [m]	3.2
Internal radius of the CS [m]	2.39
Total strain in the coil [%]	- 0.515
Maximum field on conductor [T]	13.7
Hoop stress [MPa]	527.3
Radial stress [MPa]	31.3
Vertical stress [MPa]	135.9
Tresca stress [MPa]	663.2
Central module inductance [H]	6.02
Dump time constant (for V_{max}=10kV) [s]	16.7

4.2 Hybrid CS design

A second design has been proposed for the CS1 module, based on 10 layer-wound sub-coils using HTS, R&W Nb_3Sn and NbTi conductors in the high, medium and low field sections, respectively [30]. In analogy with TF WP#1 approach, a grading of SC and SS materials is considered. Both, the hoop stress and the vertical loads are included for determining the required SS cross-section in the WP. In respect to the Nb_3Sn-based solution, the use of HTS in the inner sub-coils allows to maintain the same magnetic flux of 320 Vs in the central plane, with a higher magnetic field and a reduced outer radius of 2.813 m.

For each sub-coil, the inner radius (r_i), the radial thickness of the conductor without insulation (d_{cond}), the peak magnetic field (B_{peak}), and the current sharing temperature (T_{cs}) are listed in table 5. The conductor operation current is 50.95 kA.

Table 5. Hybrid CSWP design.

Sub-coil	Superconductor	r_i (mm)	d_{cond} (mm)	B_{peak} (T)	T_{cs} (K)
1	RE-123	1900.0	48.27	17.49	10.51
2	RE-123	2045.5	45.88	15.74	10.64
3	Nb3Sn	2169.3	51.31	14.02	6.25
4	Nb3Sn	2279.9	41.90	12.22	6.26
5	Nb3Sn	2371.7	37.40	10.45	6.25
6	Nb3Sn	2454.5	34.17	8.68	6.25
7	Nb3Sn	2530.9	30.97	6.92	6.24
8	NbTi	2600.8	38.95	5.19	6.25
9	NbTi	2687.7	27.71	3.40	6.25
10	NbTi	2750.1	27.46	1.66	6.25

Mechanical analyses, including both the hoop stress and the vertical loads, allowed to determine the required stainless steel cross-section in the winding pack. A graded design of the stainless steels conduits is proposed

since the hoop stress decreases significantly for increasing radii. The pre-magnetization current configuration is used to determine the required stainless steel fraction for each double layer. The membrane stress across the thickness of the conduits ranges between 590 and 665 MPa during this phase.

In order to estimate the required cross-section of the pre-compression tie plates, a global model including the five CS modules, the 100-mm-thick buffer plates between the modules, and the pre-compression structure has been proposed. Assuming that the superalloy Nitronic 50 is used, the minimum radial thickness for the inner and outer tie plates is 139 and 87 mm, respectively.

Thermal-hydraulic analyses have been carried out on the HTS sub-coils of the CS1 module up to the breakdown (BD), foreseen at $t = 0.8$ s after the pulse start [29]. The steep current change is expected to induce large AC losses in the SC, nevertheless ΔT_{marg}^{min} stays always above 3K.

5. HTS activity for DEMO magnets

Conductors based on High Temperature Superconductors (HTS) are under investigation to identify the benefits of this technique for future fusion power plants beyond DEMO.

REBCO tapes have been characterized both in the virgin state and after the irradiation of fast neutrons with a fluence up to $4 \cdot 10^{22}$ neutrons/m^2 [31]. The critical current is initially enhanced by irradiation, up to a turning point where I_c drops below the initial value. This critical fluence is strongly dependent on the tape and further investigation is necessary to understand the correlation between the features of the tape and its response to irradiation.

A conceptual design of TF WP based on HTS material has been proposed in 2016 [32], but the T_{hs} exceeded the 150 K criterion, and the structural analysis for jacket gave too high values for Tresca stress. To overcome this issues a new design has been proposed based on 6 Cross Conductor (CroCo) monolithic strands (10.4 mm in diameter) around 1 copper core embedded in SS jacket, as shown in figure 10(a). The main design parameters are reported in table 6. The conductor is dimensioned to carry 47.6 kA in a maximum field of 11.9 T.

The WP consists of 12 layers with 25 turns/layer, as sketched in figure 10(b). The cable dimension is unchanged for different layers, whereas the jacket thickness is constant in toroidal direction and increases in radial direction to deal with accumulated stresses.

The results of thermal-hydraulic analyses are rather encouraging with a ΔT_{marg}^{min} >10K and T_{hs} = 154K for the jacket, only slightly higher than the criterion. The 2D structural analysis for this design leads to stresses in the casing and in the jacket that are below the limits. Also, the combined shear and compression stress in the turn insulation is acceptable.

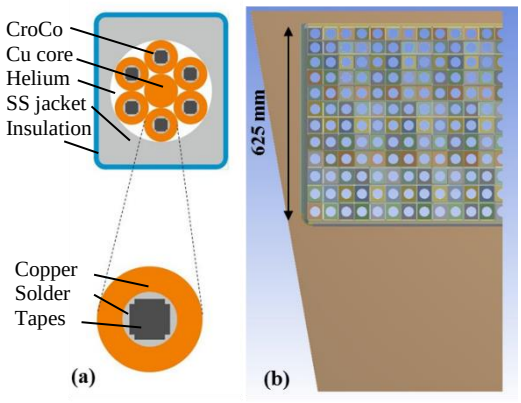

Fig. 10 (a) HTS Conductor based on CroCo strands, (b) TF WP based on HTS conductors.

Table 6. TF HTS-based reference conductor design

Parameter	Value
Number of CroCos	6 around 1 copper core
Diameter of 6 around 1 cable [mm]	31.2
Diameter of CroCo and Cu core [mm]	10.4
Copper in CroCo [mm^2]	408.28
Copper in central Cu core [mm^2]	84.95
Solder [mm^2]	56.41
REBCO in REBCO tapes [mm^2]	1.21
Silver in REBCO tapes [mm^2]	3.60
Hastelloy in REBCO tapes [mm^2]	45.00
Space for Helium cooling[mm^2]	165.4
Jacket (innermost layer) [mm^2]	954.85

Experimental tests on a smaller HTS CroCo sample [33], [34] have demonstrated a performance of about 5 kA at 4.2 K, 12 T. An extrapolation to the strand used in the TF design leads to the result that a single strand can carry about 9.45 kA at 12 T and 4.2 K, reinforcing the idea that the designed conductor has big potentiality. Finally, a 60 kA REBCO prototype conductor has been tested at 5 K, 12 T in 2015 [35]. A reduction of 15% of the I_c was observed after the electro-magnetic cycling, mostly due to a degradation at the cable edges.

New samples, based on the same concept, but properly designed for the CS inner layers, are now under manufacture and will be tested in 2018.

6. Conclusions

The design of the magnet system for DEMO tokamak is proceeding by exploring different solutions in terms of winding approaches (pancakes vs. layers) and manufacturing techniques (react & wind vs. wind & react Nb_3Sn). Experimental results show that the degradation of the conductor performances with electromagnetic cycles is absent or limited compared to most of the large-size Nb_3Sn conductors reported in literature. Also the effective strain is consistently lower, with a consequent cost saving, due to the reduced amount of superconducting material required. Critical aspects in the mechanical structure and especially on insulation have been evidenced, requiring further investigation and R&D activity. Innovative solutions based on HTS have also been proposed, in order to demonstrate their potential use in the CS coil design and

identify the benefits of this technique for future fusion power plants beyond DEMO.

Acknowledgments

This work has been carried out within the framework of the EUROfusion Consortium and has received funding from the EURATOM research and training programme 2014-2018 under grant agreement No 633053. The views and opinions expressed herein do not necessarily reflect those of the European Commission.

References

[1] F. Romanelli, Fusion Electricity, A roadmap to the realization of fusion energy, European Fusion Development Agreement, EFDA – Nov. 2012 - ISBN 978-3-00-040720-).

[2] G. Federici et al., DEMO Design Activity in Europe: Progress and Updates, *this conference* .

[3] L. Zani et al., Overview of Progress on the EU DEMO Reactor Magnet System Design, IEEE Trans. On Appl. Supercond. 26 (2016) 4204505.

[4] R. Wenninger, Reference design – 2015 April (EU DEMO1 2015) PROCESS full output, https://idm.euro-fusion.org/?uid=2MDKFH.

[5] R. Wenninger, DEMO1 - November 2013 - PROCESS output, https://idm.euro-fusion.org/?uid=2MC995.

[6] K. Sedlak et al., Design and R&D for the DEMO Toroidal Field Coils Based on Nb_3Sn React and Wind Method, IEEE Appl. Supercond. 27 (2017) 4800105.

[7] Bruzzone et al., A Prototype Conductor by React&Wind Method for the EUROfusion DEMO TF Coils, Submitted to IEEE trans on Appl. Superconductivity for MT-25.

[8] A. Panin et al., Structural Analysis of Fusion Magnets: Engineering Zooming on the Superconductor Strength, *this conference*.

[9] A. Panin, et al., Mechanical pre-dimensioning and pre-optimization of the tokamaks' toroidal coils featuring the winding pack layout, Fus. Eng. Des., in press, doi: 10.1016/j.fusengdes.2017.04.065, in press

[10] K. Sedlak, (SPC) CS and TF Winding Pack Design and Analysis, https://idm.euro-fusion.org/?uid=2MU4SH (2017)

[11] M. Lewandowska, Assessment of thermal-hydraulic properties of Winding Packs for DEMO (2017) https://idm.euro-fusion.org/?uid=2MMDVF.

[12] L. Zani and U. Fischer, Advanced definition of neutronic heat load density map on DEMO TF coils (2014) https://idm.euro-fusion.org/?uid=2MFVCA.

[13] R. Zanino et al., Common approach for thermal-hydraulic calculations (2016) available at http://www.euro-fusionscipub.org/archives/eurofusion/common-operating-values-for-demo-magnets-design-for-2016 .

[14] V. Corato et al., Common operating values for DEMO magnets design for 2016 (2016) available at http://www.euro-fusionscipub.org/archives/eurofusion/common-operating-values-for-demo-magnets-design-for-2016-2 .

[15] Muzzi et al, Design, Manufacture, and Test of an 80 kA-Class Nb_3Sn Cable-In-Conduit Conductor With Rectangular Geometry and Distributed Pressure Relief Channels, IEEE Appl. Supercond. 27 (2017) 4800206.

[16] L. Savoldi et al., Performance analysis of a graded winding pack design for the EUDEMO TF coil in normal and off-normal conditions, Fusion Engineering and Design (2017), in press.

[17] L. Savoldi et al., Quench Propagation in a TF Coil of the EU DEMO, Fusion Science and Technology 72 (2017) 439-448.

[18] B. Meszaros, EU DEMO1 2015 Plasma and equilibrium description , https://idm.euro-fusion.org/?uid=2LJFN7.

[19] M. Biancolini et al., Mechanical analysis of the ENEA TF coil proposal for the EU DEMO fusion reactor, submitted to IEEE Trans. on Appl. Supercond. (2017).

[20] A. Nijhuis et al., TF conductor samples strand thermo mechanical critical performances tests (2015) https://idm.euro-fusion.org/?uid=2M5SMM.

[21] A. Nijhuis, TF CICC conductor sample cyclic mechanical critical performance test (2016), https://idm.euro-fusion.org/?uid=2MBBBV

[22] Breschi et al., Results of the TF conductor performance qualification samples for the ITER project, Supercond. Sci. Technol. 25 (2012) 095004.

[23] A. Torre, D. Ciazynski and L. Zani, EU-DEMO TF and CS Magnet Systems Design and Analyses Performed at CEA, IEEE Transactions on Applied Superconductivity 27 (2017) 4900705.

[24] R. Vallcorba et al., Thermohydraulic analysis on CEA concept of TF and CS Coils for EU-DEMO, Submitted to IEEE trans on Appl. Superconductivity for MT-25.

[25] Q. Le Coz et al., Quench simulation of a DEMO TF coil using a quasi-3D coupling tool, Submitted to IEEE trans on Appl. Superconductivity for MT-25.

[26] Maistrello et al, Studies on DEMO Toroidal Field Circuit, submitted to IEEE TPS (2017).

[27] N. Martovetsky et al., ITER Central Solenoid Insert Test results, IEEE trans. On Applied Superconductivity 26 (2016) 4200605.

[28] L. Zani et al., Status of CEA Magnets Design Tools and Applications to EU DEMO PF and CS Magnets, Submitted to IEEE trans on Appl. Superconductivity for MT-25.

[29] M. Mattei, "DEMO AR = 3.1 preliminary Breakdown magnetic analyses," 11/08/2015.

[30] R. Wesche et al., DEMO Central Solenoid Design Based on the Use of HTS Sections at Highest Magnetic Field, Submitted to IEEE trans on Appl. Superconductivity for MT-25.

[31] M. Eisterer et al., Neutron irradiation investigation on HTS tapes, https://idm.euro-fusion.org/?uid=2N8NJV (2017)

[32] R. Heller et al., Conceptual Design Improvement of a Toroidal Field Coil for EU DEMO Using High-Temperature Superconductors, IEEE Trans. Appl. Supercond. 26 (2016) 4201105.

[33] M. J. Wolf et al., HTS CroCo: A Stacked HTS Conductor Optimized for High Currents and Long-Length Production, IEEE Trans. Appl. Supercond. 26 (2016)

6400106.
[34] M. J. Wolf et al., High current densities in small HTS CrossConductors at low temperatures and high magnetic fields, (2017) submitted to IEEE Trans. Appl. Supercond.
[35] D. Uglietti et al., Test of 60 kA coated conductor cable prototypes for fusion magnets, SUST 28 (2015) 124005.